Aeroacoustic beamforming of a model wind-turbine in anechoic and reverberant environments

Jeoffrey Fischer, Con Doolan and Branko Zajamsek

School of Manufacturing and Mechanical Engineering, UNSW Sydney, Australia

ABSTRACT

In order to obtain a better understanding of the noise radiated by wind turbines, rotors and fans, acoustic measurements were performed using a small-scale plyon-mounted rotor. The rotor, which operates at 900 RPM, is composed of 3 equally spaced NACA 0012 blades. The chord and length of the blades are 70 mm and 450 mm respectively. The pitch angle of the blades is set to either 0, 5, 10 or 15 degrees; the blades are not twisted, nor are they tapered. The rotor was placed in 2 environments: an anechoic room at the University of Adelaide and a reverberant wind tunnel test section in the UNSW aerospace research laboratory. The purpose of this paper is to investigate the effects of the hard-walls of the wind tunnel on the acoustic measurements. The acoustic radiation was measured using a 64-microphone acoustic array and processed using a conventional beamforming (CBF) algorithm. The main source of sound for all cases is located at the blade tip. The blade-plyon (or tower) interaction is clearly visible with a pitch angle of 0 degrees in the third octave [1600; 3200] Hz range. The effects of the reverberant environment are presented. While the main source is located at the same position in the two configurations, which means that acoustic measurements can be performed in the reverberant test section without any additional treatment, there are important differences between the measurements.

1. INTRODUCTION

Wind power is a renewable energy which has been increasingly developing over last few years and will keep growing in the future. Although this solution aims to reduce our consumption of other kind of energy like coal, oil or nuclear, it can however be a source of noise annoyance (Zajamsek, 2016; Doolan, 2013). Hence, understanding how noise is produced on rotating airfoils remains an important issue. It is also relevant for noise produced by aero-engine fans, propellers (for marine and aeronautical applications), ventilation fans and helicopters.

Few authors (Cho, 2010; Oerlemans, 2001) have been interested in locating noise sources on model wind-turbines. Using beamforming, which is a very popular array processing technique when locating sound sources (Mueller 2002), they observed that the noise source moves along the blade towards the tip as frequency increases.

In our work, we wish to perform acoustic tests using plyon-mounted rotors in a large, hard-walled wind tunnel section. In order to establish the effects of the reverberant field on the acoustic measurements, this paper compares acoustic source maps obtained via beamforming on the same rotor model (called a model wind-turbine in this paper) in two different environments: an anechoic room and a reverberant test-section.

2. EXPERIMENTAL SET-UP

Array measurements were performed on a model wind-turbine in an anechoic and a reverberant room. The first room was located at the University of Adelaide while the latter was located at the University of New South Wales (UNSW). The model wind-turbine, the array and the data acquisition system used were the same in each case.

2.1 Equipment

Figure 1 shows the model wind-turbine which is composed of a motor, torque measurement system, slip ring and three rotating NACA 0012 airfoils. The chord and span of each blade is respectively c = 70 mm and s = 450 mm, as shown in Figure 1. The centre of rotation of the motor is located at a height of 1.42 m and the diameter of the blades mounted is 1.1 m. The pitch angle of the rotating blades was set to $\theta = 0$, 5, 10 and 15 degrees. The spacing between the blade trailing edge and the support tower was 20 mm and guy wires were used to secure the rotor to the floor. The rotor was run at a blade-pass frequency (BPF) f_{BPF} = 45 Hz (900 rpm), which gives a blade tip speed of $V_{\mathrm{tip}} = (2\pi f_{\mathrm{BPF}} R)/N_{\mathrm{b}}$ = 52 m/s where R = 0.55 m is the radius of the blade and N_{b} = 3 stands for the number of blades. The Reynolds number based on chord at the blade tip is Re = 232,000.

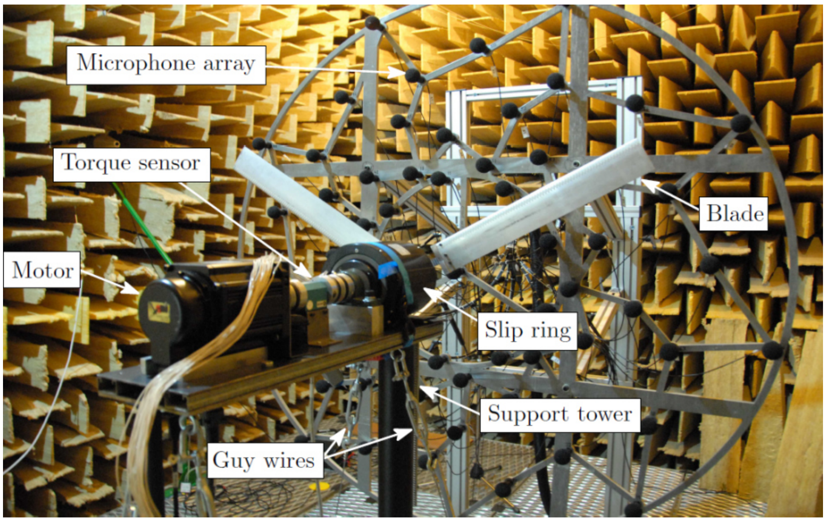

Figure 1: Picture of the wind-turbine and acoustic array in the anechoic room at University of Adelaide.

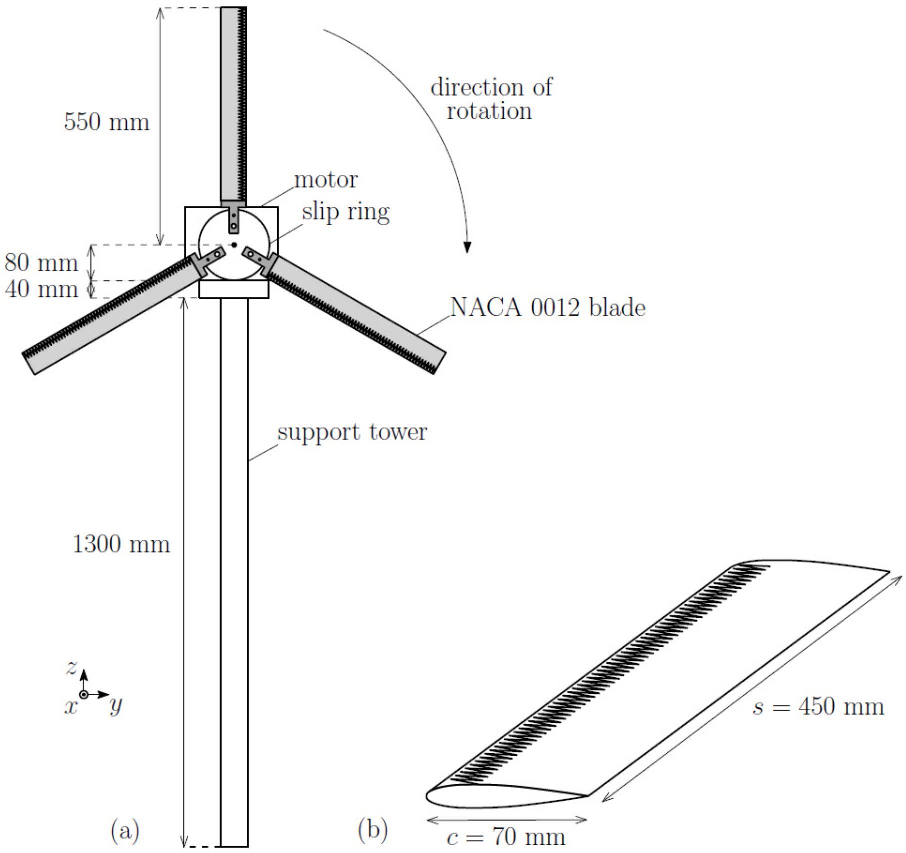

Figure 2: Schematic of the (a) model wind-turbine and (b) one of the NACA 0012 blades.

Acoustic measurements were conducted using a microphone array (see Figure 1) located in front of the wind-turbine at a different distances for the two environments (specified below). The array uses 64 G.R.A.S. 40PH phase and magnitude matched microphones, which were accurately attached to the Aluminium frame with cable glands. The microphone locations were optimised so that the array has the smallest beamwidth possible at the largest aperture possible (Prime, 2014). The array microphones were connected to a PXIe-4499 24-bit National Instrument data acquisition cards on which the data were recorded at a sampling rate of 65,536 Hz during 60 seconds.

2.2 Wind Tunnel Test Section at UNSW

The first experiment was performed in the reverberant, wind-tunnel test-section at UNSW (see Figure 3). The test-section has a regular octagon geometry with 3.05 m between the flat edges and an edge length of 1.26 m. The test section was removed from the wind tunnel to allow the array to be placed directly in front of the model. The cross-sectional area of the test section is 7.7 m^2. The array centre microphone, which could not be perfectly aligned with the centre of rotation of the wind-turbine due to some constraints in the laboratory, was located 10 cm below the axis of rotation of the turbine at a distance of d_1 = 1.4 m from the trailing edge of the rotor blades, as in the anechoic environment.

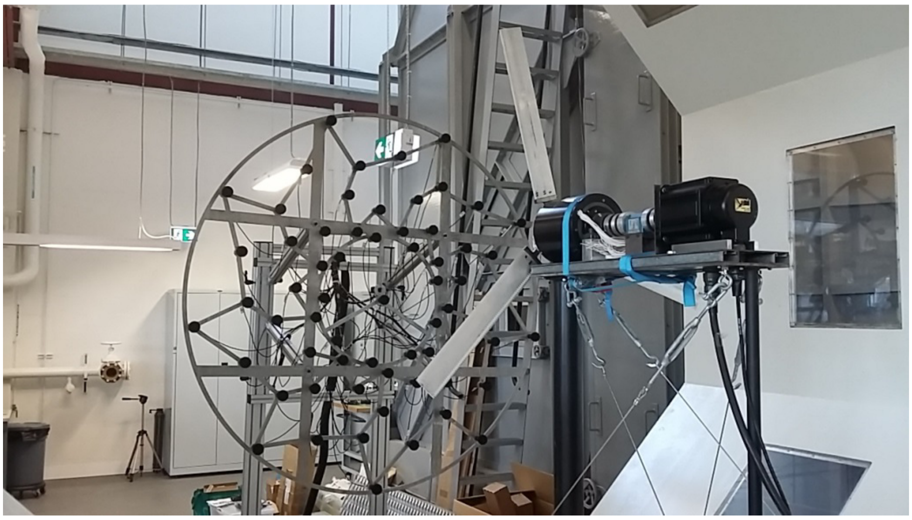

Figure 3: Picture of the wind-turbine and acoustic array in the reverberant test-section at UNSW.

2.3 Anechoic Room at University Of Adelaide

The second measurements were conducted in the anechoic room at the University of Adelaide. The room has dimensions of 4.79 m x 3.9 m x 3.94 m (73.6 m3) and provides a near-reflection free environment down to a frequency of ~100 Hz. (Zajamsek, 2014). The array was located in front of the wind-turbine at a distance of d_2 = 1.8 m and aligned along its axis of rotation.

3. BEAMFORMING

Conventional Beamforming (CBF) is a classical tool used in the field of acoustic imaging to locate noise sources (Mueller, 2002). It is based on the time-delay between the actual source and each of the microphones composing the array.

Consider a set of M microphones where the m^{th} microphone is located at $\mathbf{x_m}$. The acoustic pressure field from any given source of noise is then recorded using these microphones and projected in the frequency domain using a Fourier transform. The obtained vectors, $P(\mathbf{x_m}, f)$, are used to create the Cross-Spectral Matrix (CSM) defined as:

$$C(\mathbf{x_m}, \mathbf{x'_m}, f) = \overline{P * (\mathbf{x_m}, f)\, P(\mathbf{x'_m}, f)}\,, \tag{1}$$

where the superscript $\overline{X}$ denotes the Welch's periodogram applied to X with the use of a Hanning window function.

The CBF seeks the position of the acoustic source in a so-called focusing plane. The beamformer output at a given frequency is generally defined by:

$$Z(\mathbf{y_n}, f) = \frac{(We)^T\ C\ We}{M(M-1)}, \tag{2}$$

where $e(\mathbf{x_m}, \mathbf{y_n}, \mathrm{f})$ is called the steering vector and stands for the Green's function between the microphone located at $\mathbf{x_m}$ and the focusing point at $\mathbf{y_n}$. $W(\mathbf{x_m}, \mathbf{y_n}) = 4\pi||\mathbf{x_m} - \mathbf{y_n}||^2$ is called the weighting matrix and stands for the geometrical attenuation correction. Note that the diagonal elements of the CSM are set to 0 to improve the resolution on the beamforming map (Mueller, 2002).

In CBF, it is assumed that the acoustic sources are monopolar in nature, so the steering vector is replaced with the free-field Green's function:

$$e(\mathbf{x_m}, \mathbf{y_n}, f) = \frac{e^{-jk||\mathbf{x_m} - \mathbf{y_n}||}}{4\pi||\mathbf{x_m} - \mathbf{y_n}||}, \tag{3}$$

where $||\boldsymbol{x}||$ stands for the L^2-norm (also known as Euclidean norm) of vector $\boldsymbol{x}$ and $k = 2\pi f/c_0$ denotes the wavenumber at frequency f in a medium which speed of sound is c_0 (=340 m/s in the air at 20°C).

4. RESULTS

4.1 Spectra

As the measurements were not conducted at the same distance from the source in the two environments, the acoustic levels in the reverberant environment have been corrected using the inverse square law for acoustic propagation:

$$Lp(d_2) = Lp(d_1) + 20\log_{10}\left(\frac{d_1}{d_2}\right) = Lp(d_1) - 2.2\ dB, \tag{4}$$

where $Lp(d_i)$ is the acoustic pressure level measured at a distance d_i from the source.

The experimental spectra are presented in Figure 4 using the previous correction on the reverberant result. The low frequency peaks appearing in all the curves correspond to the BPF (= 45 Hz). These low frequency fluctuations are more intense in the reverberant environment. For frequencies below 600 Hz, the acoustic level between the two figures is slightly the same (except for the highest pitch angle), indicating that noise at these frequencies is not affected by the change of environment. However at higher frequencies, the reverberant test section provides results approximately 5 dB higher than the anechoic in the middle frequencies, up to 4 kHz. At higher frequencies, especially around 5 kHz and 9 kHz, the difference between the two curves is about 10 dB for all pitch angles.

4.2 Acoustic Maps

The acoustic maps using the beamforming procedure detailed in section 3 are now shown in Figures 5 to 8 for each pitch angle. At θ = 0°, the main noise source seems to be located at the blade tower interaction for middle frequencies f = 2 and 4 kHz. At f = 8 kHz, this source disappears leading to a more spread noise surrounding the tip region. The results obtained in the two environments are very similar, the only difference being the cleanliness of the maps.

At higher pitch angles, the middle frequencies main source is located at a different position, mainly on the right side of the figures, which corresponds to the region preceding the blade tower interaction as the rotation is clockwise. Again, the anechoic results are more accurate as the main source is recovered in a narrower region than in the reverberant case. The later results are still more polluted, especially with higher side lobe levels. Moreover, the reverberant results are similar with the anechoic ones only at the lowest frequency f = 2 kHz. At f = 4 kHz, the main noise source is spread over the tip region, possibly due to reflections from the walls. Indeed, the reverberant test-section induces image sources which are coherent with the main source and may interfere, producing more side lobes on the map. At the highest frequency f = 8 kHz, the conclusion is the same for θ = 0° and 5°, the main source being spread over the blade tip region. However at higher pitch angles, the anechoic results show a noise region preceding the blade-tower interaction region, similarly to the observations made at middle frequencies.

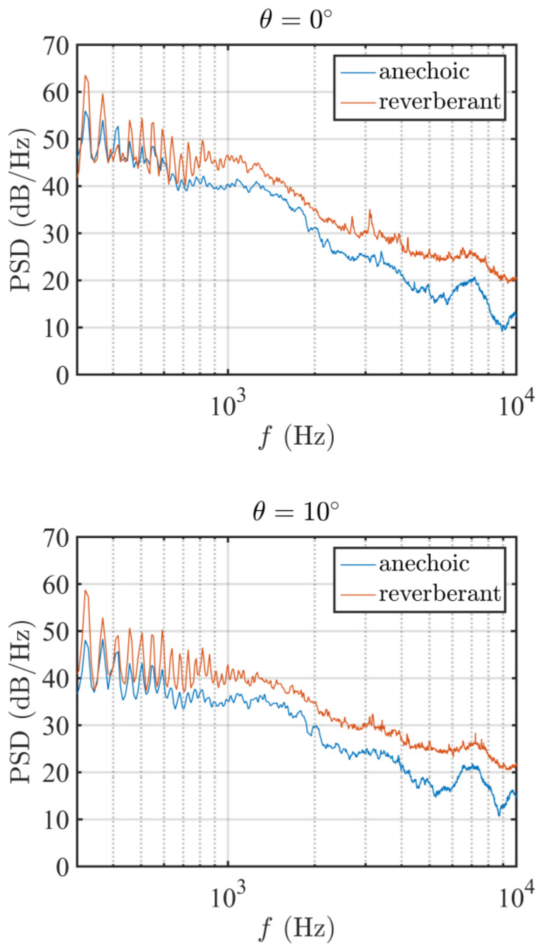

Figure 4: Spectra of the center microphone of the array in each environment for all pitch angles.

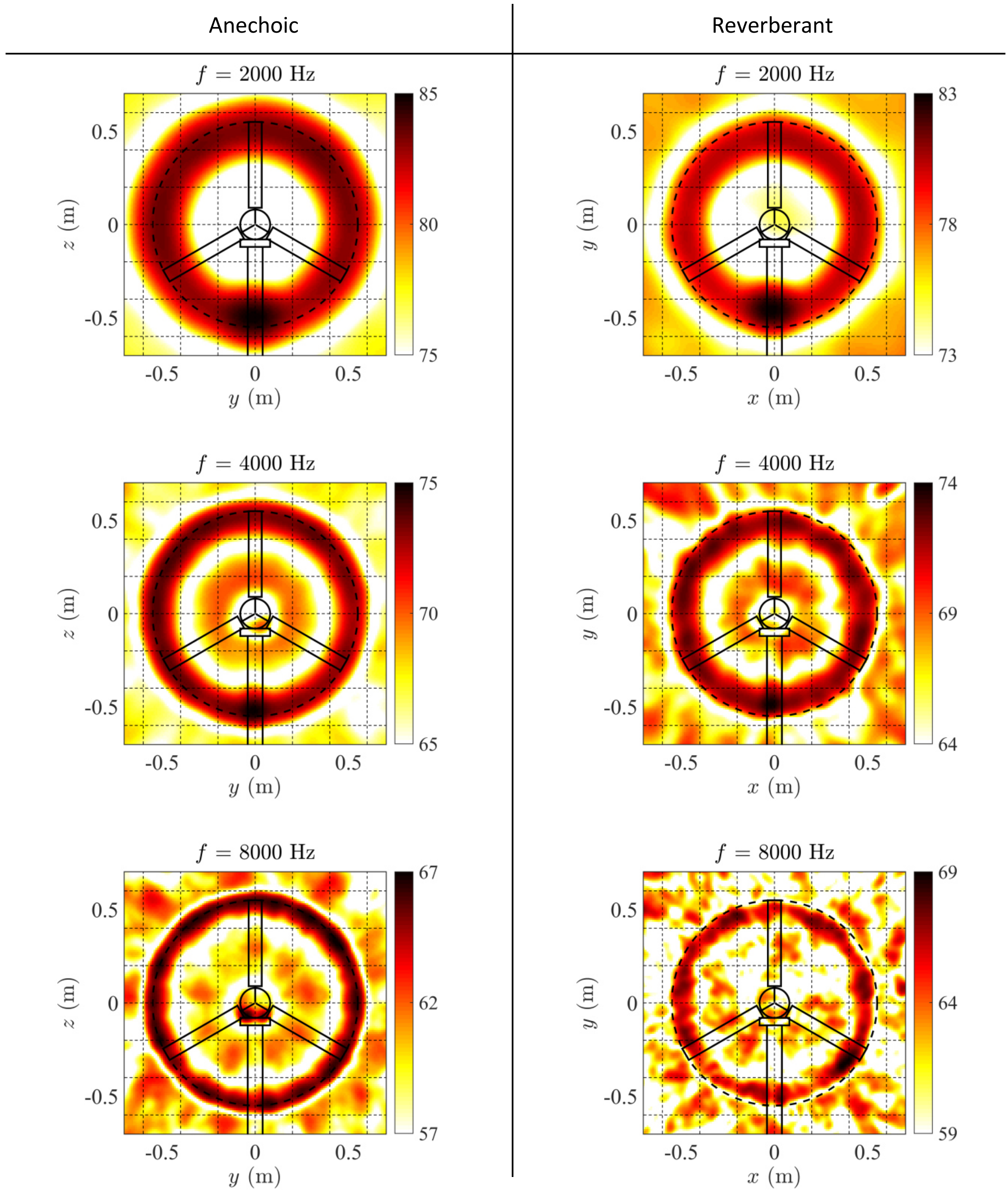

Figure 5: CBF maps of the wind-turbine noise in anechoic and reverberant environment at f = 2, 4 and 8 kHz with $\theta = 0^{\circ}$

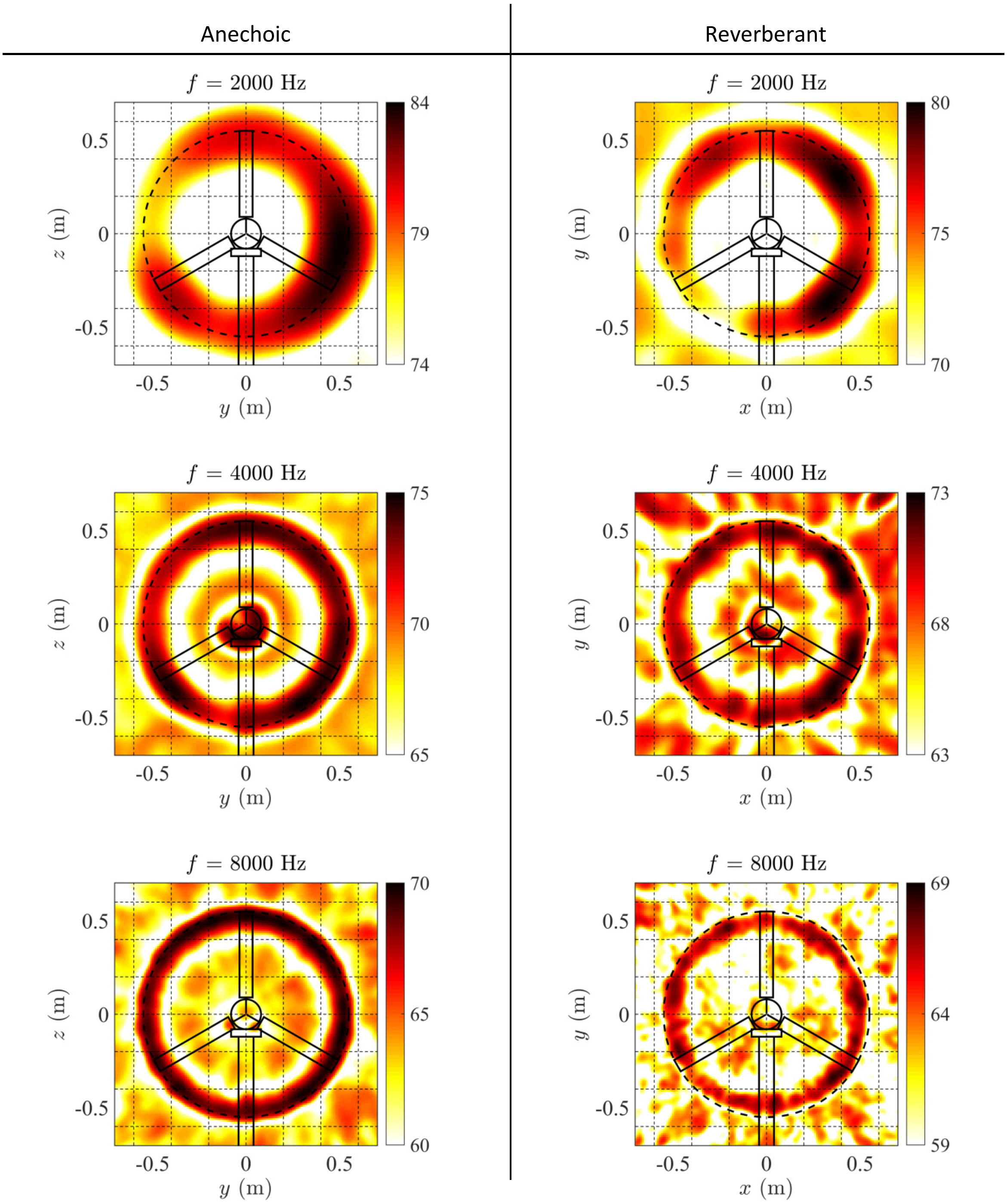

Figure 6: CBF maps of the wind-turbine noise in anechoic and reverberant environment at f = 2, 4 and 8 kHz with $\theta = 5^{\circ}$

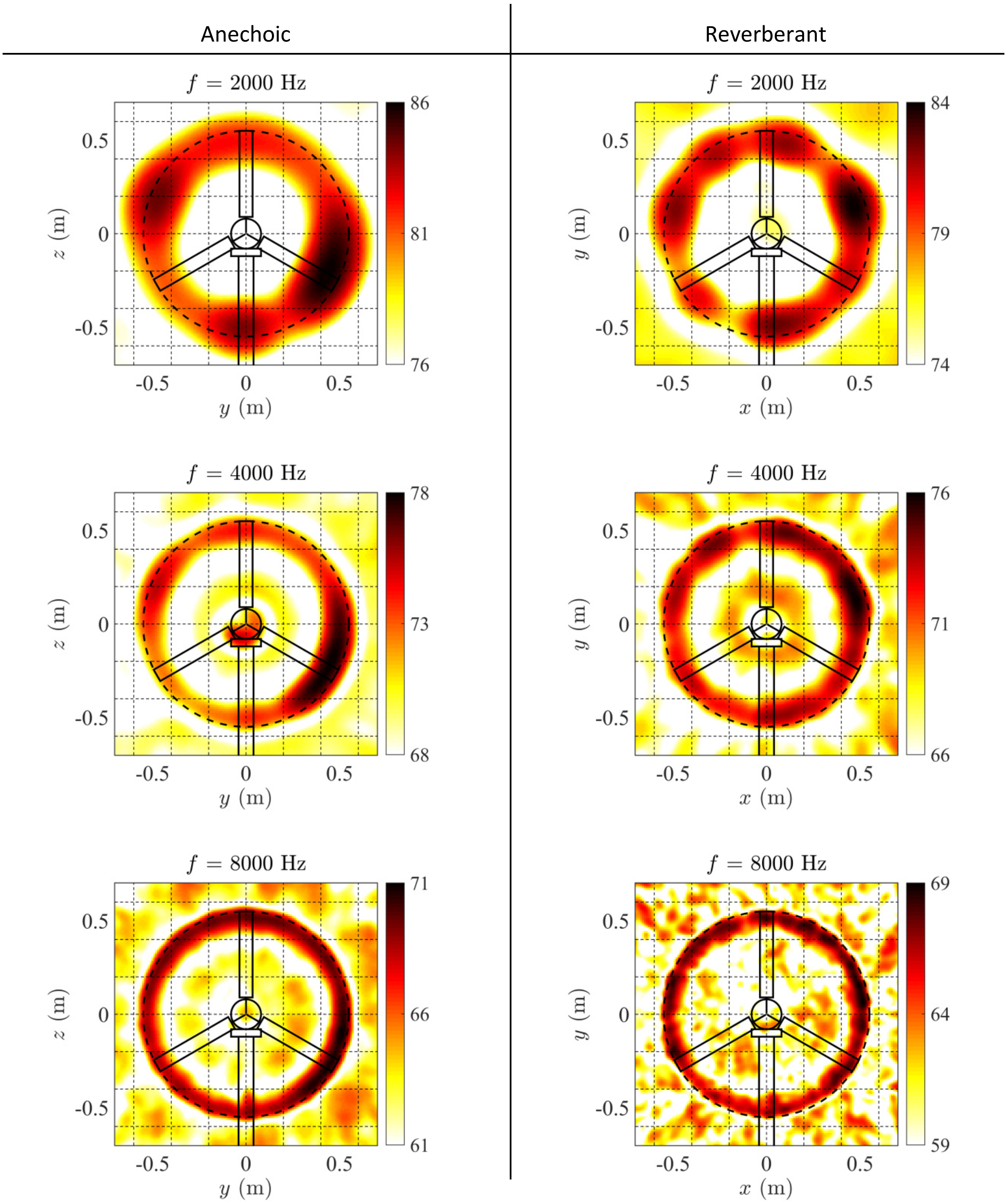

Figure 7: CBF maps of the wind-turbine noise in anechoic and reverberant environment at f = 2, 4 and 8 kHz with θ = 10^{o}

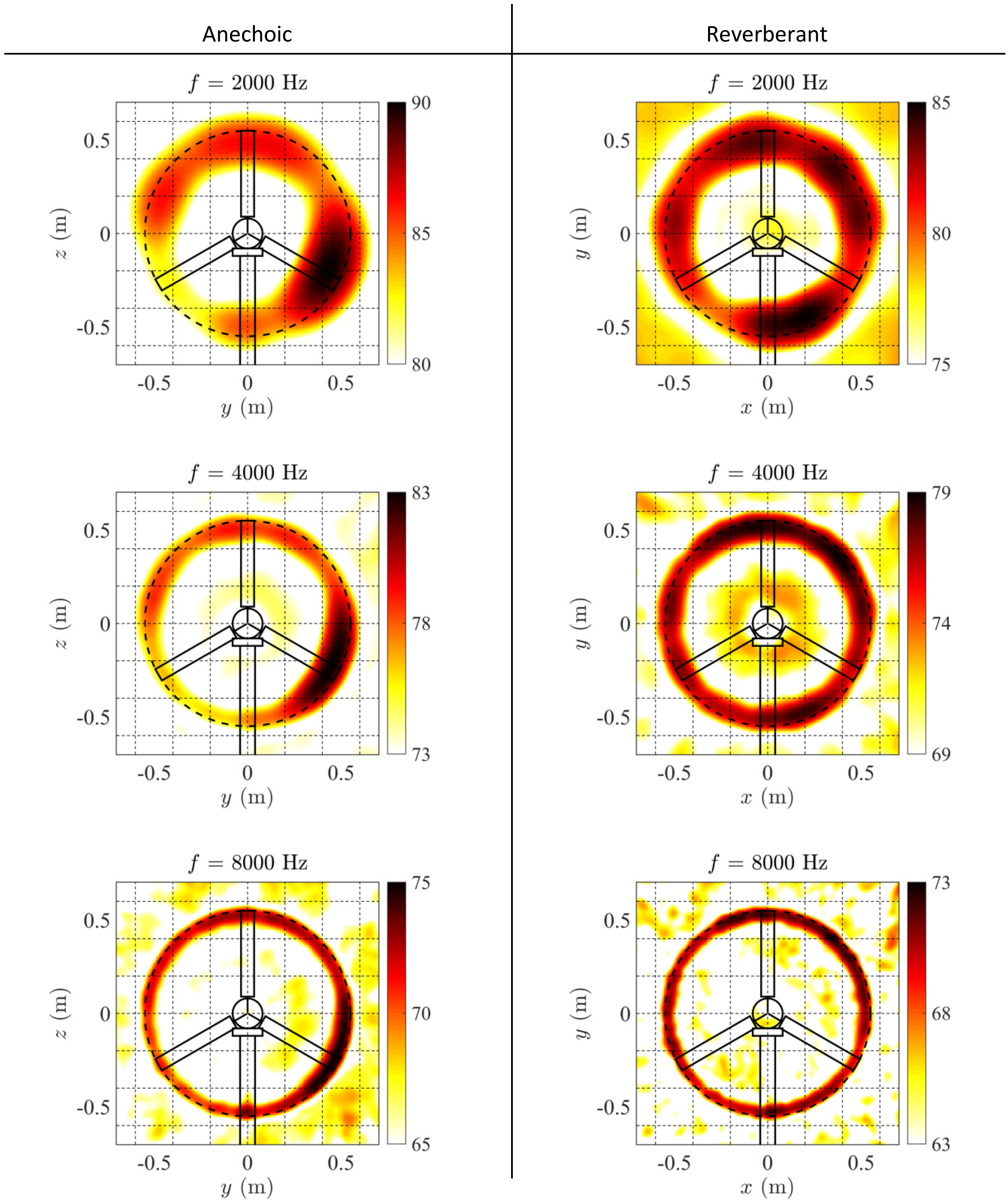

Figure 8: CBF maps of the wind-turbine noise in anechoic and reverberant environment at f = 2, 4 and 8 kHz with θ = 15°

5. CONCLUSIONS

In this work, a comparison of beamforming maps on a model wind-turbine has been presented in two different environments: an anechoic room at University of Adelaide and a reverberant test-section at UNSW.

The spectra provide similar results in the [1; 3] kHz range, but out of that band the noise recorded in the reverberant configuration is higher, especially at low frequencies where the BPF is clearly visible. At high frequencies the difference is about 5 dB.

The blade tower interaction is clearly visible on the beamforming maps at θ = 0^{o} in the mid-frequencies ranging from 2 to 4 kHz. The highest frequency shows a noise source around the blade tip region. At higher pitch angles, the main source region is located before the blade tower interaction. This result is mainly visible in the anechoic room. However, the results obtained at low frequency f = 2 kHz are similar in each environment. At higher frequencies, only the anechoic maps show the region preceding the blade tower interaction, the reverberant maps showing no predominant noise location in the circular tip region.

ACKNOWLEDGEMENTS

Financial support from the Australian Research Council, Project DP130103136, is gratefully acknowledged.

REFERENCES

Cho, T, Kim, C & Lee, D, 2010, ‘Acoustic measurement for the 12% scaled model of NREL Phase VI wind turbine’, *Current Applied Physics*, Vol 10, S320-S325.

Doolan, C 2013, ‘A review of wind turbine noise perception, annoyance and low frequency emission’, *Wind Engineering*, Vol 37(1), pp. 97-104.

Leclercq, DJJ, Doolan, CJ & Reichl, J 2007, ‘Development and validation of a small-scale anechoic wind tunnel’*,14th International Congress on Sound and Vibration*, Cairns, Australia.

Mueller, TJ 2002, *Aeroacoustic measurements,* Springer.

Oerlemans, S, Schepers, JG, Guidati, G & Wagner 2001, S, ‘Experimental demonstration of wind turbine noise reduction through optimized airfoil shape and trailing-edge serrations’, *NLR report*.

Prime, Z, Doolan, CJ & Zajamsek, B 2014, ‘Beamforming array optimisation and phase averaged sound source mapping on a model wind turbine’, *Inter-Noise and Noise-Con Congress and Conference Proceedings*, Vol. 249, pp. 1078-1086.

Zajamsek, B, Doolan, C and Prime, Z 2014, ‘Experimental measurements of rotating and stationary wind turbine rotor blade noise’, *19th Australasian Fluid Mechanics Conference*, Melbourne.

Zajamsek, B, Hansen, KL, Doolan, C & Hansen, CH 2016, ‘Characterisation of wind farm infrasound and low-frequency noise’, *Journal of Sound and Vibration*, Vol 370, pp 176-190.